Fast Legendre Spectral Method for Computing the Perturbation of a Gradient Temperature Field in an Unbounded Region due to the Presence of Two Spheres

A. Chowdhury, C. I. Christov
Department of Mathematics, University of Louisiana at Lafayette, Lafayette, Louisiana 70504

Received 5 December 2008; accepted 10 February 2009
Published online 22 June 2009 in Wiley InterScience (www.interscience.wiley.com).
DOI 10.1002/num.20479

The temperature distribution around two spheres is considered when the main field has a constant gradient at infinity. Bispherical coordinates are used, together with a transformation of the dependent variable that leads to separation of variables. Then the solution can be sought in Legendre series with respect to one of the bispherical coordinates. An important element of the proposed work is the effective way to reduce an essentially 3D problem to a set of three 2D problems. The Legendre spectral method is shown to have an exponential convergence which is confirmed by the computations. The efficiency is so high that even for the hard cases of two closely situated spheres, an accuracy of 10^{-10} is achieved with as few as 20 terms in the expansion.

Solutions with both longitudinal and transverse gradients at infinity are obtained, and the contour lines of the temperature field are presented graphically. Numer Methods Partial Differential Eq 26: 1125–1145, 2010

Keywords: Legendere-Galerkin spectral method; heat conductivity; two-sphere solution; suspensions

I. INTRODUCTION

Estimating the effective transport coefficients of heterogeneous media is of high importance for technology. The most typical example(s) of such media is (are) the particulate materials (suspensions) in which the second (particulate) phase is comprised by spherical particles (the *filler*) that are randomly dispersed throughout the continuous phase (the *matrix*). The different transport problems that can be considered for a suspension are the effective electric or heat conductivity, effective viscosity, and effective elasticity.

The first successful attempt to estimate the effective electric conductivity is due to Maxwell (see [1, p. 314]) who compared the potential created by n spheres of radius a each to the potential

Correspondence to: C. I. Christov, Department of Mathematics, University of Louisiana at Lafayette, Lafayette, LA 70504 (e-mail: christov@louisiana.edu)

of a sphere that encompasses the swarm of small spheres and has an equivalent electric conductivity in the sense of yielding the same potential at a large distance. Using this approach, Maxwell obtained the contribution to the effective conductivity of first order with respect to the volume fraction of the particulate phase. The same idea was applied by Einstein [2] for computing the first-order in volume fraction contribution to the effective viscosity of a suspension. For the elastic moduli of a suspension, the same approach was applied in [3].

Jeffrey [4] argued that the method proposed by Maxwell can give correctly only the first order in the volume fraction and went on to discuss the statistical properties of the centers of spheres. He extended the arguments from [5, 6] and justified the conclusion that the second order approximation in the volume fraction can be obtained only if the solution around two spheres is obtained. A comprehensive review of the work on viscosity of suspensions can be found in [7].

The method of functional expansions (Volterra–Wiener series) with random point basis function (RPF) for rigorous treatment of the statistical properties of materials with random structure has been originated in [8]. The application to estimating the effective heat conduction modulus of monodisperse suspension was presented in [9], while the elastic moduli were treated in [10]. After the generalization of the RPF expansion to marked random point functions was outlined in [11], the most general case of a polydisperse suspension of perfect disorder type became amenable to the Volterra–Wiener method (see [12]). Nowadays, it can be considered as proved that the two-sphere solution does rigorously lead to the second-order approximation with respect to the volume fraction as it gives precisely the second-order kernel in the formal Volterra–Wiener expansion. Since the effective transport properties are aimed at, one needs to solve the two-sphere problem under constant gradient of the main field at infinity. This defines the main goal of this article: to develop an efficient numerical tool for solving the two-sphere problem.

A method to solve the Laplace equation, called currently "twin-pole expansion" (see [4]) was proposed by Hicks [13]. The method consists in expanding the solution in spherical harmonics around two poles. This method was used on numerous occasions. Its main advantage lies in the fact that the integrals needed to compute the overall transport coefficients are easy to evaluate. For this reason, Jeffrey [4] went on to suggest that, in the context of the statistical theory of suspension, the twin-pole expansion is superior to the method involving bispherical coordinates. This claim is not immediately verifiable because the twin-pole expansion actually involves two levels of approximation: the first level is the truncation of the Legendre series. The second level of approximation stems from the fact that the functional coefficients of the series which depend on the radial coordinate, cannot be found in closed form. Rather, the solution is sought in asymptotic series with respect to the small parameter a/R, where a is the radius of the bigger of the spheres, and R is the distance between their centers.

The procedure of asymptotic solution can be interpreted physically as adding to the solution created by the boundary condition on one of the boundaries, a solution that is reflected from the other boundary. The procedure is currently known as "method of reflections" [14]. It has been successfully applied in various problems with two boundaries. For Stokes flow around a sphere in a cylindrical pipe, see [15]. For the problem of settling velocity of a group of particles in a Stokes' flow, see [16].

For the case of closely situated spheres when one of the radii is much greater than the other, the said parameter can actually tend to unity, which can make the respective series very slowly convergent. The bispherical coordinates offer an approach that is free of this limitation.

Without belittling the importance of the twin-pole expansion, a numerical solution with controlled convergence is still in demand, if for no other reason, but at least for estimating the region of convergence of the twin-pole expansion. The approach based on bispherical coordinates gives the solution in closed form albeit in infinite series with respect to Legendre polynomials. As it will

be shown in this article, the convergence of this series is exponential which reduces the number of needed terms to two to three dozens at most. To shed light on this subject, we limit ourselves to the problem of temperature field as it is somewhat simpler in implementation than viscosity or elasticity.

A successful numerical (e.g., spectral) solution is contingent on finding the appropriate curvilinear coordinates in which the boundaries of the domain of the solution are coordinate lines. The fact that the bispherical coordinates are the best suited tool for solving a transport problem in a medium containing two spherical solutions was first emphasized by Lord Kelvin. He was apparently the first to introduce the bispherical coordinates in 1846 in a letter to Liouville (see [17, pp. 211–212]).

The first detailed application of the bispherical coordinates for solving the Laplace equation was given by Jeffery [18] for the potential flow around two spheres. The important difference here is that the temperature field under consideration has a linear gradient at infinity. The application of the bispherical coordinates to the heat conduction problem around two spheres with constant gradient at infinity was sketched in [19], but no numerical results were presented. This article deals with the numerical implementation of the expansion proposed in [19].

II. POSING THE PROBLEM

To formulate the problem of heat conduction in a medium containing two spherical inclusions, we define first the characteristic function of an spherical inclusion of radius a as follows

$$h(\boldsymbol{x};a)=\begin{cases}0 & \text{for } |\boldsymbol{x}|>a,\\ 1 & \text{for } |\boldsymbol{x}|\le a.\end{cases}$$

Then one can consider a medium which has a discontinuous coefficient of heat diffusion, namely

$$\varkappa=\varkappa_{\mathrm{m}}+\sum_j [\![\varkappa]\!]\, h(\boldsymbol{x}-\boldsymbol{x}_j;a), \tag{1}$$

where $\varkappa_{\mathrm{m}}$ is the heat conductivity coefficient of the matrix, $\varkappa_{\mathrm{f}}$ is the heat conductivity coefficient of the filler, and $[\![\varkappa]\!] \stackrel{\mathrm{def}}{=} \varkappa_{\mathrm{f}}-\varkappa_{\mathrm{m}}$. Respectively, $\boldsymbol{x}_j$ is the spatial position of the center of each spherical inclusion. The properties of the suspension under consideration depend essentially on the multipoint probability distributions of the centers of the inclusions.

Consider now a temperature field which has a constant gradient at infinity, say $\boldsymbol{G}$. The perturbation due to a single inclusion centered at the origin of the coordinate system is given by

$$T_1(\boldsymbol{x};a)=\begin{cases}-\beta\boldsymbol{G}\cdot\boldsymbol{x} & \text{for } |\boldsymbol{x}|\le a,\\ -\beta\frac{a^3}{|\boldsymbol{x}|^3}\boldsymbol{G}\cdot\boldsymbol{x} & \text{for } |\boldsymbol{x}|>a,\quad \beta=\frac{[\![\varkappa]\!]}{\varkappa_f+2\varkappa_m}.\end{cases} \tag{2}$$

In a similar fashion, one can treat the perturbation due to the presence of two spheres. The temperature in an unbounded medium can be considered as a superposition of the linear field and the perturbation, $T_2(\boldsymbol{x},z;a,b)$, introduced by the presence of the two spherical inclusions, namely

$$T(\boldsymbol{x},z;a,b)=\boldsymbol{G}\cdot\boldsymbol{x}+T_2(\boldsymbol{x},z;a,b). \tag{3}$$

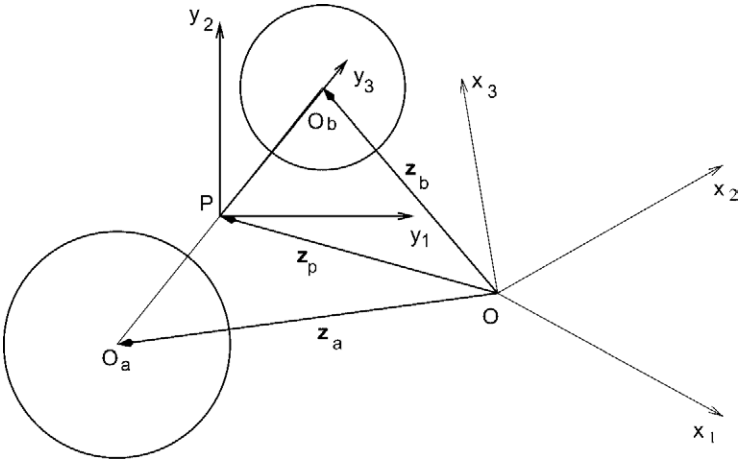

FIG. 1. Relation between bispherical and Cartesian coordinates.

It is convenient to introduce also the so-called "pure interaction," S, as the addition to the sum of the perturbations introduced by the two spheres, when the latter are considered to be alone in the matrix, namely

$$T_2(\boldsymbol{x}, z; a, b) = T_{11}(\boldsymbol{x}, z; a, b) + S(\boldsymbol{x}, z; a, b), \quad T_{11}(\boldsymbol{x}, z; a, b) \stackrel{\text{def}}{=} T_1(\boldsymbol{x}; a) + T_1(\boldsymbol{x} - z; b). \quad (4)$$

Here, T_{11} is the superposition of two one-sphere solutions centered at two different spatial points.

Now, for the perturbation field, T_2, we have the following equation with discontinuous coefficient

$$\nabla \cdot [\varkappa_{\mathrm{m}} \nabla T_2 + [\![\varkappa]\!]\, [h(\boldsymbol{x}; a) + h(\boldsymbol{x} - z; b)](G + \nabla T_2)] = 0, \quad (5)$$

In its virtue of being an equation with discontinuous coefficient, Eq. (5) is equivalent to three different Laplace equations (see Fig. 1):

$$\varkappa_{\mathrm{f}} \nabla^2 T_2^{(1)} = 0 \quad \text{for } |\boldsymbol{x}| \le a, \quad (6a)$$

$$\varkappa_{\mathrm{f}} \nabla^2 T_2^{(2)} = 0 \quad \text{for } |\boldsymbol{x} - z| \le b, \quad (6b)$$

$$\varkappa_{\mathrm{m}} \nabla^2 T_2^{(0)} = 0 \quad \text{for } (|\boldsymbol{x}| > a) \cap (|\boldsymbol{x} - z| > b). \quad (6c)$$

The total temperature function, T, must be continuous since no point heat sources are allowed. In addition, the heat flux across the spheres' boundaries has to be also continuous. Then the temperature functions, $T_2^{(i)}$ that are the solutions of the above three equations, are to match continuously at the common boundaries of their regions. Respectively, the normal derivative of T_2, has

to experience a "jump" in order that the total flux is continuous. The aforementioned requirements for continuity give the boundary conditions to be satisfied

$$T_2^{(0)} = T_2^{(1)}, \quad \varkappa_{\mathrm{m}} \left[\frac{\partial T_2^{(0)}}{\partial n} + \boldsymbol{G} \cdot \boldsymbol{n} \right] = \varkappa_{\mathrm{f}} \left[\frac{\partial T_2^{(1)}}{\partial n} + \boldsymbol{G} \cdot \boldsymbol{n} \right] \quad \text{for } |\boldsymbol{x}| = a, \tag{7a}$$

$$T_2^{(0)} = T_2^{(2)}, \quad \varkappa_{\mathrm{m}} \left[\frac{\partial T_2^{(0)}}{\partial n} + \boldsymbol{G} \cdot \boldsymbol{n} \right] = \varkappa_{\mathrm{f}} \left[\frac{\partial T_2^{(2)}}{\partial n} + \boldsymbol{G} \cdot \boldsymbol{n} \right] \quad \text{for } |\boldsymbol{x} - \boldsymbol{z}| = b, \tag{7b}$$

where $\boldsymbol{n}$ stands for the outward normal vector to the spheres and $\frac{\partial T}{\partial n}$ denotes the derivative in normal direction, and a and b are the radii of the spheres.

A further simplification gives:

$$T_2^{(0)} = T_2^{(1)}, \quad \varkappa_{\mathrm{m}} \frac{\partial T_2^{(0)}}{\partial n} = \varkappa_{\mathrm{f}} \frac{\partial T_2^{(1)}}{\partial n} + [\![\varkappa]\!] \, \boldsymbol{G} \cdot \boldsymbol{n} \quad \text{for } |\boldsymbol{x}| = a, \tag{8a}$$

$$T_2^{(0)} = T_2^{(2)}, \quad \varkappa_{\mathrm{m}} \frac{\partial T_2^{(0)}}{\partial n} = \varkappa_{\mathrm{f}} \frac{\partial T_2^{(2)}}{\partial n} + [\![\varkappa]\!] \, \boldsymbol{G} \cdot \boldsymbol{n} \quad \text{for } |\boldsymbol{x} - \boldsymbol{z}| = b. \tag{8b}$$

Since T_2 is a perturbation, then it must vanish at infinity, i.e.,

$$T_2^{(0)} \to 0 \quad \text{at } |\boldsymbol{x}| \to \infty \quad \text{and} \quad \boldsymbol{z} \quad \text{arbitrary}. \tag{9}$$

III. BI-SPHERICAL COORDINATES

The bispherical coordinate system offers an important advantage in treating this problem, since both boundaries $|\boldsymbol{x}| = a$ and $|\boldsymbol{x} - \boldsymbol{z}| = b$ can be represented as coordinate surfaces. To introduce the bispherical coordinates, one must first change to another set of Cartesian coordinates centered at a point, P, that lies on the segment connecting the centers of the spheres. Let $Ox_1x_2x_3$ is a general Cartesian coordinate system, and $\boldsymbol{z}_a$ and $\boldsymbol{z}_b$ are the position vectors of the centers of the spheres. We choose the coordinate line y_3 to be collinear with the line connecting the centers of spheres. Figure 1 gives the idea of how the new Cartesian system $Py_1y_2y_3$ is constructed. The actual connection between the two Cartesian coordinate systems is important only when the solution presented here will be used in finding the second-order terms in the expression of the effective heat-conduction modulus. For the purposes of this work, it is enough to mention that in terms of the new system, $Py_1y_2y_3$, the asymptotic boundary condition reads

$$T(\boldsymbol{y}) \simeq \hat{T} + \boldsymbol{E} \cdot \boldsymbol{y}, \quad \text{for } |\boldsymbol{y}| \to \infty. \tag{10}$$

Here $\hat{T}$ is some constant that depends on the relative positions of the centers O and P, while the new gradient is given by

$$\boldsymbol{E} = \mathbb{A}\boldsymbol{G}, \tag{11}$$

where $\mathbb{A}$ is the Jacobian matrix of coordinate transformation.

Now the connection between the Cartesian coordinates $Py_1y_2y_3$ and bispherical ones ξ, η, ζ may be expressed as follows:

$$y_1 = c\frac{\sin\xi}{\cosh\eta - \cos\xi}\cos\zeta, \quad y_2 = c\frac{\sin\xi}{\cosh\eta - \cos\xi}\sin\zeta, \quad y_3 = c\frac{\sinh\eta}{\cosh\eta - \cos\xi}, \tag{12}$$

where c is called focal distance. The ranges of the bispherical coordinates are $0 \leq \xi < \pi$, $-\infty < \eta < +\infty$ and $0 \leq \zeta < 2\pi$. The focal distance and the coordinates of the two spheres, η_a, η_b can be evaluated from the known lengths: distance between spheres $z = |z_b - z_a|$, the radii of the spheres a, b as follows

$$c = \frac{\sqrt{z^4 + b^4 + a^4 - 2z^2b^2 - 2a^2b^2 - 2z^2a^2}}{2z} = \sqrt{\alpha^2 z^2 - a^2}, \tag{13}$$

$$\eta_a = -\ln\left|\frac{c}{a} + \sqrt{1 + \frac{c^2}{a^2}}\right| \equiv -\operatorname{arcsinh}\frac{c}{a}, \tag{14}$$

$$\eta_b = \ln\left|\frac{c}{b} + \sqrt{1 + \frac{c^2}{b^2}}\right| \equiv \operatorname{arcsinh}\frac{c}{b}, \tag{15}$$

$$\alpha = \frac{z^2 - b^2 + a^2}{2z^2}. \tag{16}$$

The last quantity is positive since $z > a + b$ is the expression of the fact that the spheres do not intersect each other. Without loosing the generality, we have chosen $\eta_a < 0$.

For the relative distances of the sphere's centers from the point P, we get

$$d_a = \frac{1}{z}\sqrt{c^2 + b^2}, \quad d_b = \frac{1}{z}\sqrt{c^2 + b^2}, \quad d_a + d_b = 1. \tag{17}$$

Making use of the last formula, we are able to complete the connection of systems $Py_1y_2y_3$ and $Ox_1x_2x_3$ by specifying the "offset vector"

$$z_p = z_a + d_a z = (1 - d_a)z_a + d_a z_b = d_b z_a + (1 - d_b)z_b. \tag{18}$$

To express the result in Cartesian coordinates for possible further manipulation and presentation, we also need the inverse transformation, namely we express ξ, η, and ζ in terms of y_1, y_2, and y_3. By doing so, one has to be very careful with the regions where the bispherical coordinates may be multivalued. After some algebra, we obtain

$$\eta = \operatorname{arccoth}\left(\frac{y_1^2 + y_2^2 + y_3^2 + c^2}{2cy_3}\right) \tag{19a}$$

$$\xi = \arcsin\left[\sqrt{\frac{4c^2\left(y_1^2 + y_2^2\right)}{\left(y_1^2 + y_2^2 + (y_3 + c)^2\right)\left(y_1^2 + y_2^2 + (y_3 - c)^2\right)}}\right] \tag{19b}$$

$$\zeta = \begin{cases} \arcsin\left(y_2/\sqrt{y_1^2 + y_2^2}\right), & y_1 > 0, \\ \pi - \arcsin\left(y_2/\sqrt{y_1^2 + y_2^2}\right), & y_1 < 0, \\ \dfrac{1}{2}\pi, & y_1 = 0. \end{cases} \tag{19c}$$

IV. THE BOUNDARY-VALUE PROBLEM

Each of the Laplace equations (6) have the following form in terms of bispherical coordinates

$$\Delta\Phi \equiv \frac{(\cosh\eta-\cos\xi)^3}{c^2\sin\xi}\left[\frac{\partial}{\partial\eta}\left(\frac{\sin\xi}{\cosh\eta-\cos\xi}\frac{\partial\Phi}{\partial\eta}\right)+\frac{\partial}{\partial\xi}\left(\frac{\sin\xi}{\cosh\eta-\cos\xi}\frac{\partial\Phi}{\partial\xi}\right)+\frac{1}{\sin\xi(\cosh\eta-\cos\xi)}\frac{\partial^2\Phi}{\partial\zeta^2}\right], \quad (20)$$

where Φ stands for the functions $T_2^{(0)}, T_2^{(1)}$, or $T_2^{(2)}$. It is well seen that the variable ζ does not enter the coefficients of Eq. (20), i.e., it is a cyclic variable of the Laplace operator in bispherical coordinates. One also notes that the outward normal derivative $\frac{\partial}{\partial n}$ is, in fact, a partial derivative with respect to η at $\eta=\eta_a$ and with respect to $(-\eta)$ at $\eta=\eta_b$. Respectively, the outward normal vector n is equal to e_η or $-e_\eta$, where e_η is the unit vector tangential to η-coordinate line.

The unit vector e_η is easily expressed in terms of unit vectors $\boldsymbol{y}_1^0$, $\boldsymbol{y}_2^0$, and $\boldsymbol{y}_3^0$ of the auxiliary coordinate system as follows:

$$\boldsymbol{e}_\eta = -\frac{\sin\xi\sinh\eta\cos\zeta}{\cosh\eta-\cos\xi}\boldsymbol{y}_1^0 - \frac{\sin\xi\sinh\eta\sin\zeta}{\cosh\eta-\cos\xi}\boldsymbol{y}_2^0 - \frac{\cosh\eta\cos\xi-1}{\cosh\eta-\cos\xi}\boldsymbol{y}_3^0. \quad (21)$$

Then

$$\boldsymbol{E}\cdot\boldsymbol{n} = sgn(\eta)E_\eta, \quad E_\eta = \frac{E_1\sin\xi\sinh\eta\cos\zeta + E_2\sin\xi\sinh\eta\sin\zeta + E_3(\cosh\eta\cos\xi-1)}{\cosh\eta-\cos\xi}, \quad (22)$$

where E_j are the components of vector $\boldsymbol{E}$ defined in (11). Let us now denote

$$R^{(i)}(\xi,\eta,\zeta;c,\theta,\varphi) \equiv T_2^{(i)}(x_1,x_2,x_3,z_1,z_2,z_3), \quad i=0,1,2. \quad (23)$$

Obviously, each $R^{(i)}$ satisfies Eq. (20). The boundary conditions expressing the continuity of the temperature field and the heat flux read

$$R^{(0)} = R^{(1)}, \quad \varkappa_{\mathrm{m}}\frac{\partial R^{(0)}}{\partial\eta} = \varkappa_{\mathrm{f}}\frac{\partial R^{(1)}}{\partial\eta} - [\![\varkappa]\!]\frac{c}{\cosh\eta-\cos\xi}E_\eta \quad \text{for } \eta=\eta_a, \quad (24a)$$

$$R^{(0)} = R^{(2)}, \quad \varkappa_{\mathrm{m}}\frac{\partial R^{(0)}}{\partial\eta} = \varkappa_{\mathrm{f}}\frac{\partial R^{(2)}}{\partial\eta} + [\![\varkappa]\!]\frac{c}{\cosh\eta-\cos\xi}E_\eta \quad \text{for } \eta=\eta_b. \quad (24b)$$

To the boundary conditions at spheres' surfaces, Eq. (24), one has to add also the asymptotic boundary conditions (a.b.c.), which in terms of bispherical coordinates read

$$R^{(0)} \to 0 \quad \text{at } \xi,\eta \to 0. \quad (25)$$

Note that the change of sign in (24a) stems from (22) because $\eta_a < 0$. For the sake of reducing the complexity of notations, we introduce the functions

$$U(\xi,\eta) = \frac{c}{\cosh\eta_a-\cos\xi}E_{\eta_a} \quad \text{and} \quad V(\xi,\eta) = \frac{c}{\cosh\eta_b-\cos\xi}E_{\eta_b}. \quad (26)$$

V. REDUCTION OF THE 3D B.V.P. TO THREE 2D B.V.P.'S

The main idea of the original work [19] was to reduce the 3D problem to a set of three 2D problems making advantage of the fact that ζ appears to be what is called "cyclic variable" and it enters the picture only through the boundary conditions. The form of the Eqs. (24a) and (24b) hints at the idea that one can seek the solutions of the 3D problems in the form of the following linear combinations:

$$R^{(i)}(\xi,\eta,\zeta) = R_0^{(i)}(\xi,\eta) + R_1^{(i)}(\xi,\eta)\cos\zeta + R_2^{(i)}(\xi,\eta)\sin\zeta \quad \text{for } i = 0,1,2. \tag{27}$$

The equation for the newly introduced functions are

$$\frac{\partial}{\partial\eta}\left(\frac{\sin\xi}{\cosh\eta-\cos\xi}\frac{\partial R_j^{(i)}}{\partial\eta}\right) + \frac{\partial}{\partial\xi}\left(\frac{\sin\xi}{\cosh\eta-\cos\xi}\frac{\partial R_j^{(i)}}{\partial\xi}\right) - a_j\frac{R_j^{(i)}}{\sin\xi(\cosh\eta-\cos\xi)} = 0, \tag{28}$$

where $a_0 = 0, a_1 = a_2 = 1$.

In the same manner, the boundary conditions are manipulated. On assuming that

$$U(\xi,\eta) = U_0(\xi,\eta) + U_1(\xi,\eta)\cos\zeta + U_2(\xi,\eta)\sin\zeta,$$
$$V(\xi,\eta) = V_0(\xi,\eta) + V_1(\xi,\eta)\cos\zeta + V_2(\xi,\eta)\sin\zeta,$$

one derives

$$U_0 = cE_3\frac{\cosh\eta_a\cos\xi-1}{(\cosh\eta_a-\cos\xi)^2}, \quad U_j = cE_j\frac{\sin\xi\sinh\eta_a}{(\cosh\eta_a-\cos\xi)^2}, \quad j = 1,2, \tag{29a}$$

$$V_0 = cE_3\frac{\cosh\eta_b\cos\xi-1}{(\cosh\eta_b-\cos\xi)^2}, \quad V_j = cE_j\frac{\sin\xi\sinh\eta_b}{(\cosh\eta_b-\cos\xi)^2}, \quad j = 1,2, \tag{29b}$$

and then Eq. (24) can be recast as follows

$$R_j^{(0)} = R_j^{(1)}, \quad \varkappa_{\mathrm{m}}\frac{\partial R_j^{(0)}}{\partial\eta} = \varkappa_{\mathrm{f}}\frac{\partial R_j^{(1)}}{\partial\eta} - [\![\varkappa]\!]\,U_j \quad \text{for } \eta = \eta_a, \quad j = 0,1,2. \tag{30a}$$

$$R_j^{(0)} = R_j^{(2)}, \quad \varkappa_{\mathrm{m}}\frac{\partial R_j^{(0)}}{\partial\eta} = \varkappa_{\mathrm{f}}\frac{\partial R_j^{(2)}}{\partial\eta} + [\![\varkappa]\!]\,V_j \quad \text{for } \eta = \eta_b, \quad j = 0,1,2. \tag{30b}$$

Respectively, the boundary condition at infinity (25) yields

$$R_j^{(0)} \to 0 \quad \text{at } \xi,\eta \to 0, \quad j = 0,1,2. \tag{31}$$

So far, for $i = 0,1,2$ and $j = 0,1,2$, we have nine boundary value problems for evaluating the nine functions $R_j^{(i)}$. The important achievement here is that these boundary value problems are two-dimensional.

VI. SEPARATION OF VARIABLES

It is well known that by means of the substitution

$$R_j^{(i)} = \sqrt{2(\cosh\eta - \cos\xi)}A_j^{(i)}, \tag{32}$$

Equation (28) can be transformed into an equation with separating variables:

$$\frac{\partial^2 A_j^{(i)}}{\partial\eta^2} + \frac{\partial^2 A_j^{(i)}}{\partial\xi^2} + \cot\xi\frac{\partial A_j^{(i)}}{\partial\xi} - \frac{1}{4}A_j^{(i)} - \frac{a_j}{\sin^2\xi}A_j^{(i)} = 0. \tag{33}$$

In terms of functions $A_j^{(i)}$, the boundary conditions (30a) and (30b) adopt the form:

$$\varkappa_{\mathrm{m}}(\cosh\eta_a - \mu)\left.\frac{\partial A_j^{(0)}}{\partial\eta}\right|_{\eta=\eta_a} + \frac{1}{2}\varkappa_{\mathrm{m}}\sinh\eta_a A_j^{(0)} = \varkappa_{\mathrm{f}}(\cosh\eta_a - \mu)\left.\frac{\partial A_j^{(1)}}{\partial\eta}\right|_{\eta=\eta_a}$$
$$+ \frac{1}{2}\varkappa_{\mathrm{f}}\sinh\eta_a A_j^{(1)} - \frac{1}{2}[\![\varkappa]\!]\,\bar{U}_j, \quad A_j^{(0)}(\xi,\eta_a) = A_j^{(1)}(\xi,\eta_a), \quad j = 0,1,2. \tag{34a}$$

$$\varkappa_{\mathrm{m}}(\cosh\eta_b - \mu)\left.\frac{\partial A_j^{(0)}}{\partial\eta}\right|_{\eta=\eta_b} + \frac{1}{2}\varkappa_{\mathrm{m}}\sinh\eta_b A_j^{(0)} = \varkappa_{\mathrm{f}}(\cosh\eta_b - \mu)\left.\frac{\partial A_j^{(2)}}{\partial\eta}\right|_{\eta=\eta_b}$$
$$+ \frac{1}{2}\varkappa_{\mathrm{f}}\sinh\eta A_j^{(2)} + \frac{1}{2}[\![\varkappa]\!]\,\bar{V}_j, \quad A_j^{(0)}(\xi,\eta_b) = A_j^{(2)}(\xi,\eta_b), \quad j = 0,1,2. \tag{34b}$$

where

$$\bar{U}_0 = \sqrt{2(\cosh\eta_a - \cos\xi)} = \sqrt{2}cE_3\frac{\mu\cosh\eta_a - 1}{(\cosh\eta_a - \mu)^{3/2}}, \tag{35a}$$

$$\bar{V}_0 = \sqrt{2(\cosh\eta_b - \cos\xi)} = \sqrt{2}cE_3\frac{\mu\cosh\eta_b - 1}{(\cosh\eta_b - \mu)^{3/2}}, \tag{35b}$$

$$\bar{U}_{1,2} = \sqrt{2(\cosh\eta_a - \cos\xi)} = cE_{1,2}\frac{\sqrt{1-\mu^2}\sinh\eta_a}{(\cosh\eta_a - \mu)^{3/2}}, \tag{35c}$$

$$\bar{V}_{1,2} = \sqrt{2(\cosh\eta_b - \cos\xi)} = cE_{1,2}\frac{\sqrt{1-\mu^2}\sinh\eta_b}{(\cosh\eta_b - \mu)^{3/2}}. \tag{35d}$$

Let us now seek the solution of (33) in the form

$$A_j^{(i)}(\xi,\eta) = B_j^{(i)}(\xi)H_j^{(i)}(\eta). \tag{36}$$

Then each of Eq. (33) breaks into two-independent equations

$$\frac{d^2}{d\eta^2}H_j^{(i)}(\eta) = \lambda^2 H_j^{(i)}(\eta), \tag{37a}$$

$$\frac{d^2}{d\xi^2}B_j^{(i)} + \cot\xi\frac{d}{d\xi}B(i)_j + \left(\lambda^2 - \frac{1}{4}\right)B_j^{(i)} - \frac{a_j}{\sin^2\xi}B_j^{(i)} = 0. \tag{37b}$$

Consider first the last equation. Let us denote

$$B_j^{(i)}(\xi) = D_j^{(i)}(\mu) \quad \text{where } \mu = \cos\xi. \tag{38}$$

Then (37b) immediately transforms to the following :

$$(1-\mu^2)\frac{d^2}{d\mu^2}D_j^{(i)} - 2\mu\frac{d}{d\mu}D_j^{(i)} + \left[\left(\lambda^2 - \frac{1}{4}\right) - \frac{a_j}{1-\mu^2}\right]D_j^{(i)} = 0, \tag{39}$$

which is the well-known Legendre equation. Its solutions that do not possess singularities, are the Legendre polynomials $P^{a_j}_{\lambda-\frac{1}{2}}$ with $\lambda - \frac{1}{2}$ being a positive integer, namely

$$D_j^{(i)} = P_n^{a_j}(\mu), \tag{40}$$

where it has already been acknowledged that $\sqrt{a_j} = a_j$. For $a_j = 0$ these are the Legendre polynomials and for $a_j = 1$ they are the associated Legendre polynomials. Both kinds of polynomials are defined for positive integers $n = \lambda - \frac{1}{2} > 0$ and therefore the fundamental solution of (37a) are the exponential functions $H_j^{(i)}(\eta) = e^{\pm(n+\frac{1}{2})}$.

VII. THE METHOD OF GENERATING FUNCTION

The general solution for $A_j^{(i)}$ is given by the following sum

$$A_j^{(i)} = \sum_{n=0}^{\infty}\left[L_{ij}^{(n)}e^{\left(n+\frac{1}{2}\right)\eta} + M_{ij}^{(n)}e^{-\left(n+\frac{1}{2}\right)\eta}\right]P_n^{a_j}(\mu). \tag{41}$$

The form of the boundary conditions Eqs. (34a) and (34b) requires that the functions in the right-hand side of Eq. (35) are represented into Legendre series. The main idea is to make use of the generating function for Legendre polynomials [19]. To establish the connection to the generating function, we begin with $\bar{U}_0$ which can be expressed as

$$\bar{U}_0 = \sqrt{2}cE_3\frac{\mu\cosh\eta_a - 1}{(\cosh\eta_a - \mu)^{3/2}} = 2cE_3e^{\frac{3}{2}\eta_a}\frac{\mu(1+t^2) - 2t}{t(1+t^2-2\mu t)^{3/2}}, \quad t \stackrel{\text{def}}{=} e_a^{\eta} < 1. \tag{42}$$

The expression on the right-hand side of the last equation can be expanded into Legendre series, if the generating function of Legendre polynomials (cf. [18, Section 3.6]) is used. The latter is defined as follows

$$G(t,\mu) \stackrel{\text{def}}{=} (1-2t\mu+t^2)^{-1/2} = \sum_{n=0}^{\infty}t^nP_n(\mu) \quad \text{for } t < 1. \tag{43}$$

For the derivative of the generating function one gets

$$\frac{\partial G(t,\mu)}{\partial t} = \frac{(\mu - t)}{(1-2t\mu+t^2)^{3/2}} = \sum_{n=0}^{\infty}nt^{n-1}P_n(\mu). \tag{44}$$

A linear combination of Eqs. (43) and (44) gives the Legendre series of the r.h.s. of Eq. (42), namely

$$2cE_3e^{\frac{3}{2}\eta_a}\frac{\mu(1+t^2)-2t}{t(1+t^2-2\mu t)^{3/2}} = 2cE_3e^{\frac{1}{2}\eta_a}\left[-G(t,\mu)+\left(\frac{1}{t}-t\right)G_t(t,\mu)\right].$$

The last relation gives us the expansion of $\bar{U}_0$:

$$\bar{U}_0 = 2cE_3e^{\frac{3}{2}\eta_a}\sum_{n=0}^{\infty}\left[-(n+1)e^{n\eta_a}+ne^{(n-2)\eta_a}\right]P_n(\mu). \tag{45a}$$

In a similar fashion, we derive the expansion for $\bar{V}_0$:

$$\bar{V}_0 = 2cE_3e^{-\frac{3}{2}\eta_b}\sum_{n=0}^{\infty}\left[-(n+1)e^{-n\eta_b}+ne^{-(n-2)\eta_b}\right]P_n(\mu). \tag{45b}$$

The only difference now is that $t = e^{-\eta_b} < 1$.

The expansions for functions $\bar{U}_j$ and $\bar{V}_j$, involve the associated Legendre polynomials of first order $P_n^1(\mu)$. The generating function in this case is defined as

$$G^1(t,u) \equiv \frac{t(1-\mu^2)^{1/2}}{(1-2t\mu+t^2)^{3/2}} = \sum_{n=1}^{\infty}t^nP_n^1(\mu). \tag{46}$$

Then, after applying the latter to the respective Eq. (35), we obtain

$$\bar{U}_{1,2} = 4cE_{1,2}\frac{t(1-\mu^2)^{1/2}}{(1-2t\mu+t^2)^{3/2}} = 4cE_{1,2}e^{\frac{1}{2}\eta_a}\sinh\eta_a\sum_{n=1}^{\infty}e^{n\eta_a}P_n^1(\mu), \quad t=e^{\eta_a}, \tag{47a}$$

$$\bar{V}_{1,2} = 4cE_{1,2}\frac{t(1-\mu^2)^{1/2}}{(1-2t\mu+t^2)^{3/2}} = 4cE_{1,2}e^{\frac{-1}{2}\eta_b}\sinh\eta_b\sum_{n=1}^{\infty}e^{-n\eta_b}P_n^1(\mu), \quad t=e^{-\eta_b}. \tag{47b}$$

To satisfy the boundary conditions, we need to expand into Legendre series also the terms of the type $(\cosh\eta-\mu)P_n^{a_j}$ which enter Eq. (41). Making use of the relation [20, Section 3.9]

$$(\cosh\eta-\mu)P_n^{a_j}(\mu) = -\frac{n+a_j}{2n+1}P_{n-1}^{a_j}+\cosh\eta P_n^{a_j}-\frac{n+1-a_j}{2n+1}P_{n+1}^{a_j}, \tag{48}$$

we arrive, e.g., for $A_j^{(0)}$ to the following :

$$\begin{aligned}(\cosh\eta-\mu)&\frac{\partial A_j^{(0)}}{\partial\eta}\\ &=\sum_{n=0}^{\infty}\left[(n+1/2)e^{(n+1/2)\eta}\left(-\frac{n+1+a_j}{2n+1}e^{\eta}L_{0j}^{(n+1)}+\cosh\eta L_{0j}^{(n)}-\frac{n-a_j}{2n+1}e^{-\eta}L_{0j}^{(n-1)}\right)\right.\\ &\left.-(n+1/2)e^{-(n+1/2)\eta}\left(-\frac{n+1+a_j}{2n+1}e^{-\eta}M_{0j}^{(n+1)}+\cosh\eta M_{0j}^{(n)}-\frac{n-a_j}{2n+1}e^{\eta}M_{0j}^{(n-1)}\right)\right]P_n^{a_j}.\end{aligned} \tag{49}$$

It should be noted here that because of their coefficients, the terms containing $L_{ij}^{(-1)}$ and $M_{ij}^{(-1)}$ vanish identically, which leaves the system coupled.

An important reduction of the number of unknowns is achieved when acknowledging the requirement of no singularities at focal points. This requires that the coefficients of the diverging terms must vanish identically

$$L_{2j}^{(n)} = 0, \quad M_{1j}^{(n)} = 0, \quad j = 0, 1, 2, \quad n = 0, 1, 2. \tag{50}$$

Note that the boundary condition at infinity (25) is automatically satisfied due to the specific form of the substitution (32) and to the fact that $A_j^{(i)}$ exhibit no singularities at $\xi = \eta = 0$.

Now, satisfying the conditions for continuity of the temperature field across the spheres' surfaces [part of Eq. (34)], we get

$$L_{1j}^{(n)} = L_{0j}^{(n)} + e^{-(2n+1)\eta_a} M_{0j}^{(n)}, \tag{51a}$$

$$M_{2j}^{(n)} = e^{(2n+1)\eta_b} L_{0j}^{(n)} + M_{0j}^{(n)}. \tag{51b}$$

Next, we introduce the expansion (41) into those equations from (34) that deal with the continuity of the flux, acknowledge (51), and get the following algebraic system for the nontrivial coefficients

$$\begin{aligned}
&[\![\varkappa]\!]\left[-(n+1+a_j)e^{-\eta_b} M_{0j}^{(n+1)} + [2n\cosh\eta_b + e^{-\eta_b}] M_{0j}^{(n)} - (n-a_j)e^{\eta_b} M_{0j}^{(n-1)}\right] \\
&\quad + \{\varkappa\}\left[-(n+1+a_j)e^{\eta_b} L_{0j}^{(n+1)} + [(2n+1)\cosh\eta_b] L_{0j}^{(n)} - (n-a_j)e^{-\eta_b} L_{0j}^{(n-1)}\right] e^{(2n+1)\eta_b} \\
&\qquad - [\![\varkappa]\!]\sinh\eta_b e^{(2n+1)\eta_b} L_{0j}^{(n)} = \begin{cases} -4c[\![\varkappa]\!]\, E_3\left[n\sinh\eta_b - \frac{1}{2}e^{-\eta_b}\right], & j = 0, \\ -4c[\![\varkappa]\!]\, E_j \sinh\eta_b, & j = 1, 2. \end{cases}
\end{aligned} \tag{52a}$$

$$\begin{aligned}
&[\![\varkappa]\!]\left[-(n+1+a_j)e^{\eta_a} L_{0j}^{(n+1)} + [2n\cosh\eta_a + e^{\eta_a}] L_{0j}^{(n)} - (n-a_j)e^{-\eta_a} L_{0j}^{(n-1)}\right] \\
&\quad + \{\varkappa\}\left[-(n+1+a_j)e^{-\eta_a} M_{0j}^{(n+1)} + [(2n+1)\cosh\eta_a] M_{0j}^{(n)} - (n-a_j)e^{\eta_a} M_{0j}^{(n-1)}\right] e^{-(2n+1)\eta_a} \\
&\qquad + [\![\varkappa]\!]\sinh\eta_a e^{-(2n+1)\eta_a} M_{0j}^{(n)} = \begin{cases} -4c[\![\varkappa]\!]\, E_3\left[n\sinh\eta_a + \frac{1}{2}e^{\eta_a}\right], & j = 0, \\ 4c[\![\varkappa]\!]\, E_j \sinh\eta_a, & j = 1, 2. \end{cases}
\end{aligned} \tag{52b}$$

where $\{\varkappa\} \stackrel{\text{def}}{=} \varkappa_m + \varkappa_f$.

By multiplying (52a) by $e^{-(2n+1)\eta_b}$, and Eq. (52b) by $e^{(2n+1)\eta_a}$, we get

$$\begin{aligned}
&[\![\varkappa]\!]\left[-(n+1+a_j)e^{-(2n+2)\eta_b} M_{0j}^{(n+1)} + [2n\cosh\eta_b + e^{-\eta_b}] e^{-(2n+1)\eta_b} M_{0j}^{(n)} - (n-a_j)e^{-2n\eta_b} M_{0j}^{(n-1)}\right] \\
&\quad + \{\varkappa\}\left[-(n+1+a_j)e^{\eta_b} L_{0j}^{(n+1)} + [(2n+1)\cosh\eta_b] L_{0j}^{(n)} - (n-a_j)e^{-\eta_b} L_{0j}^{(n-1)}\right] \\
&\qquad - [\![\varkappa]\!]\sinh\eta_b L_{0j}^{(n)} = \begin{cases} -4c[\![\varkappa]\!]\, E_3\left[n\sinh\eta_b - \frac{1}{2}e^{-\eta_b}\right] e^{-(2n+1)\eta_b}, & j = 0, \\ -4c[\![\varkappa]\!]\, E_j \sinh\eta_b e^{-(2n+1)\eta_b}, & j = 1, 2. \end{cases}
\end{aligned} \tag{53a}$$

$$\begin{aligned}
&[\![\varkappa]\!]\left[-(n+1+a_j)e^{(2n+2)\eta_a} L_{0j}^{(n+1)} + [2n\cosh\eta_a + e^{\eta_a}]\, e^{(2n+1)\eta_a} L_{0j}^{(n)} - (n-a_j)e^{2n\eta_a} L_{0j}^{(n-1)}\right] \\
&\quad + \{\varkappa\}\left[-(n+1+a_j)e^{-\eta_a} M_{0j}^{(n+1)} + [(2n+1)\cosh\eta_a] M_{0j}^{(n)} - (n-a_j)e^{\eta_a} M_{0j}^{(n-1)}\right] \\
&\qquad + [\![\varkappa]\!]\sinh\eta_a M_{0j}^{(n)} = \begin{cases} -4c[\![\varkappa]\!]\, E_3\left[n\sinh\eta_a + \frac{1}{2}e^{\eta_a}\right] e^{(2n+1)\eta_a}, & j = 0, \\ 4c[\![\varkappa]\!]\, E_j \sinh\eta_a e^{(2n+1)\eta_a}, & j = 1, 2. \end{cases}
\end{aligned} \tag{53b}$$

Systems (53a) and (53b) are closed for evaluating the coefficients $L_{0j}^{(n)}$ and $M_{0j}^{(n)}$. This resulting coupled system is sparse with a double-tri-diagonal structure that gives a significant advantage if a large number of terms is to be retained in the series. However, the fast exponential convergence of the algorithm allows one to use <20 terms in the series, which means that the efficiency of the solver to be used is irrelevant.

VIII. CONVERGENCE AND VALIDATIONS

Using the Rodrigues formula (see [21]), it can be shown that for the standardized Legendre polynomials ($P_n(0) = 1$) the following expressions hold: for the coefficients of the Legendre series (see [22])

$$f(z) = \sum_{n=0}^{\infty} a_n P_n(z), \quad a_n = \frac{2n+1}{2^{n+1}n!} \int_{-1}^{1} f^{(n)}(x)(1-x^2)^n dx.$$

The last formula ensures exponential convergence for the series when the sought function is analytic (all derivative up to infinite order exist). We should stress the point here that the functions $A(\mu)$ are analytic despite of the fact that we are dealing with an equation with discontinuous coefficients. This is due to the advantage presented by the bispherical coordinates, which are structured in a way that makes the discontinuity to take place only in the first derivatives of functions that depend on the variable η. The first task to perform here is to verify the practical convergence of our spectral method.

We consider a case when the filler has dimensionless heat conductivity coefficient $\varkappa_{\mathrm{f}} = 2$ which is larger than the conductivity of the matrix =1.

The exponential convergence ensures that retaining 10–20 terms in the series should prove to be a sufficient number for quantitatively very good approximation. For the sake of testing, the practical convergence, we focus on the following two main cases:

1. $z = 15, a = 3, b = 2$;
2. $z = 6, a = 3, b = 2$.

For the in-depth validation of the algorithm, it is important to have spheres of different radii. In case 1, the distance between the spheres is largely relative to their radii. The expectation is that such a case will be easier in some sense and that the solution will resemble closely the mere superposition T_{11} of the two one-sphere solutions. In case 2, the distance between the closest points of the spheres is one unit which is twice smaller than the radius of the smaller sphere. In terms of the dimensionless distance $a/z = 1/2$, we see that the small parameter is not anymore really small.

In Fig. 2, we present the computed coefficients, $L_{00}^{(n)}, M_{00}^{(n)}$, versus their number, and compare them with best-fit curves of exponential type. Figure 2(a) shows the convergence for large distance between the spheres (case 1), whereas Fig. 2(b) shows the result for case 2 when the spheres are close to each other.

Each of the subfigures have two panels: the first one shows the solution for nontrivial longitudinal temperature gradient $E_3 = 1$ and $E_{2,3} = 0$, whereas the second panel shows the case of nontrivial lateral temperature gradient $E_1 = 1$ and $E_{2,3} = 0$. It is important to treat the longitudinal and lateral gradients separately, because the former case involves Legendre polynomials, whereas the latter involves the associated Legendre polynomials. The most important conclusion from

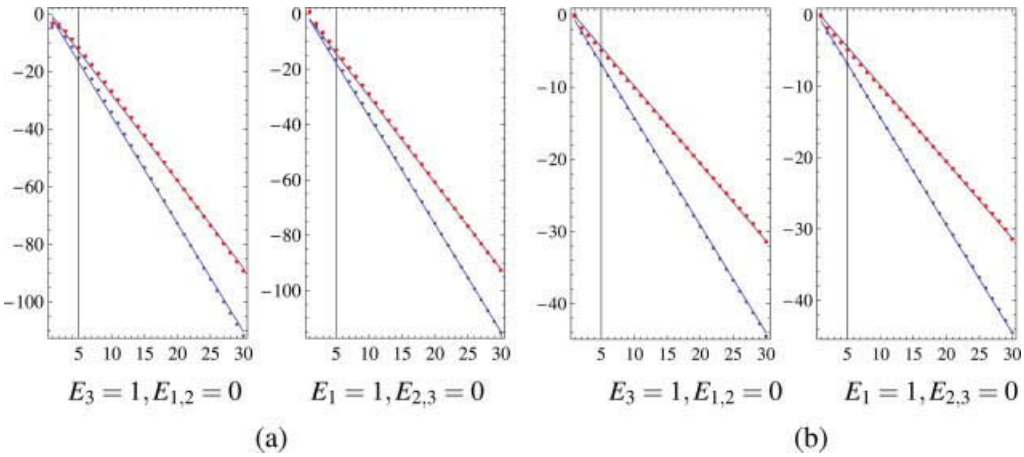

FIG. 2. Exponential decay of the computed coefficients $L_{00}^{(n)}$ (upper line) and $M_{00}^{(n)}$ (lower line). (a) Distance $z = 15$ between spheres. Best-fit: $7 \cdot 2^{-5.4n}$ and $9 \cdot 2^{-4.35n}$. (b) Distance $z = 6$ between spheres. Best-fit: $2 \cdot 2^{-2.15n}$ and $2.5 \cdot 2^{-1.55n}$. [Color figure can be viewed in the online issue, which is available at www.interscience.wiley.com.]

the results presented in Fig. 2 is that the exponential convergence is unequivocally confirmed by the computations. Actually, the practical convergence is very slightly super-exponential. Another conclusion that is not intuitively expected is that the actual numbers for the convergence rates of the two types of series (ordinary and associate Legendre polynomials) are the same, and the best-fit lines have the same slopes in the logarithmic plots.

The conclusion of this validation study is that the Legendre spectral series do converge exponentially and present a very efficient method for solving the problem under consideration. For case 1, the method needs just 10 terms to give accuracy of 10^{-20}. For case 2, the convergence is somewhat slower, but the accuracy of 10^{-20} can be achieved with only 20 terms.

IX. RESULTS AND DISCUSSION

We begin the discussion of the results with presenting the longitudinal cross-section of the computed profile. For the sake of demonstration, we chose the case of nontrivial longitudinal temperature gradient, $E_3 = 1$ and $E_{1,2} = 0$. Figure 3 presents the longitudinal profile of T_2 together with the superposition of two one-sphere solutions, T_{11}. One can see that for case 1, the two profiles differ very little. This outlines the limits of the necessity of the two-sphere solution. It is interesting to observe that even in case 2 when the distance is relatively small, the maximal deviation of the two-sphere solution, T_2, from T_{11} is $<25\%$. However, some characteristics that depend on the gradients may deviate more. This already speaks in favor of expecting a good quantitative approximation from the method of reflections for moderate distances between the spheres.

A. Large Distance Between Spheres

In case 1, the deviation from the superposition of two one-sphere solutions is more pronounced for the case of a longitudinal temperature gradient. For this reason, we present in Fig. 4 the result

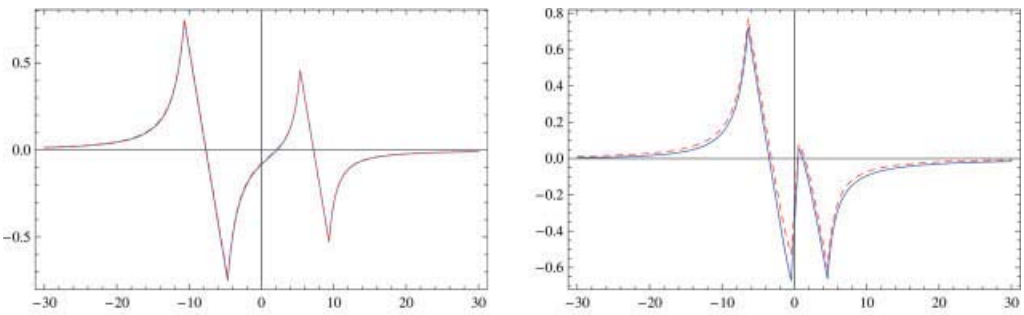

FIG. 3. Temperature profiles (solid lines) as function of the longitudinal coordinate y_3 for the case $E_3 = 1$ and $E_{1,2} = 0$. The dashed lines give the profile of the superposition of the one-sphere solutions, T_{11}. The solid line presents T_2. [Color figure can be viewed in the online issue, which is available at www.interscience.wiley.com.]

for the longitudinal gradient. Because of the obvious symmetry in this case, we can show the result in the plane y_3, y_1 with y_3 playing the role of the abscissa. The top panel (a) of Fig. 4 shows the solution obtained here, which is the disturbance to the main linear distribution created by the two spheres. The middle panel (b) gives the full temperature profile. One can clearly see that the gradient inside the spheres is smaller (the contour lines are sparser) than outside because $\varkappa_{\mathrm{f}} = 2 > 1 = \varkappa_{\mathrm{m}}$. It is also seen that the temperature gradient experiences a jump across the spheres' surfaces.

The lowest panel (c) shows what we call the "pure perturbation," i.e., the deformation of the one-sphere fields due to the presence of the other sphere. In fact, what is presented in Fig. 4(c) is the difference between the two-sphere solution and the superposition of two one-sphere solutions, $S = T_2 - T_{11}$. The maximum of the modulus of T_2 in panel (a) is $\approx$0.66, whereas the maximum of the modulus of S in panel (c) is $\approx$0.0146, which makes the amplitude of the pure perturbation about 2.2% of the amplitude of the total perturbation.

B. Small Distance Between Spheres

Next, we explore the temperature distribution for two closely situated spheres. We present the result in Fig. 5 following the same order of the panels as in the previous figure. The left panels are for the case of purely longitudinal gradient, whereas the right panels pertain to the case of purely transverse gradient.

Once again, the overall maximum of the modulus of the total perturbation is of order of 0.6, but this time it is situated at the lee side of the smaller sphere for the case of longitudinal gradient. The maximum of the modulus S is of order of 0.15, putting the pure perturbation roughly at 25% of the full perturbation, which is of order of magnitude larger than for the case of well separated spheres.

C. Combined Longitudinal and Transverse Gradients

After we have elucidated the behavior of the solutions in two purely 2D situations, we move to the case of combined gradients at infinity, namely $E_3 = 1$ and $E_1 = 1$. We can keep $E_2 = 0$ because the presence of nontrivial E_2 alongside with a nontrivial E_1 simply rotates the patterns

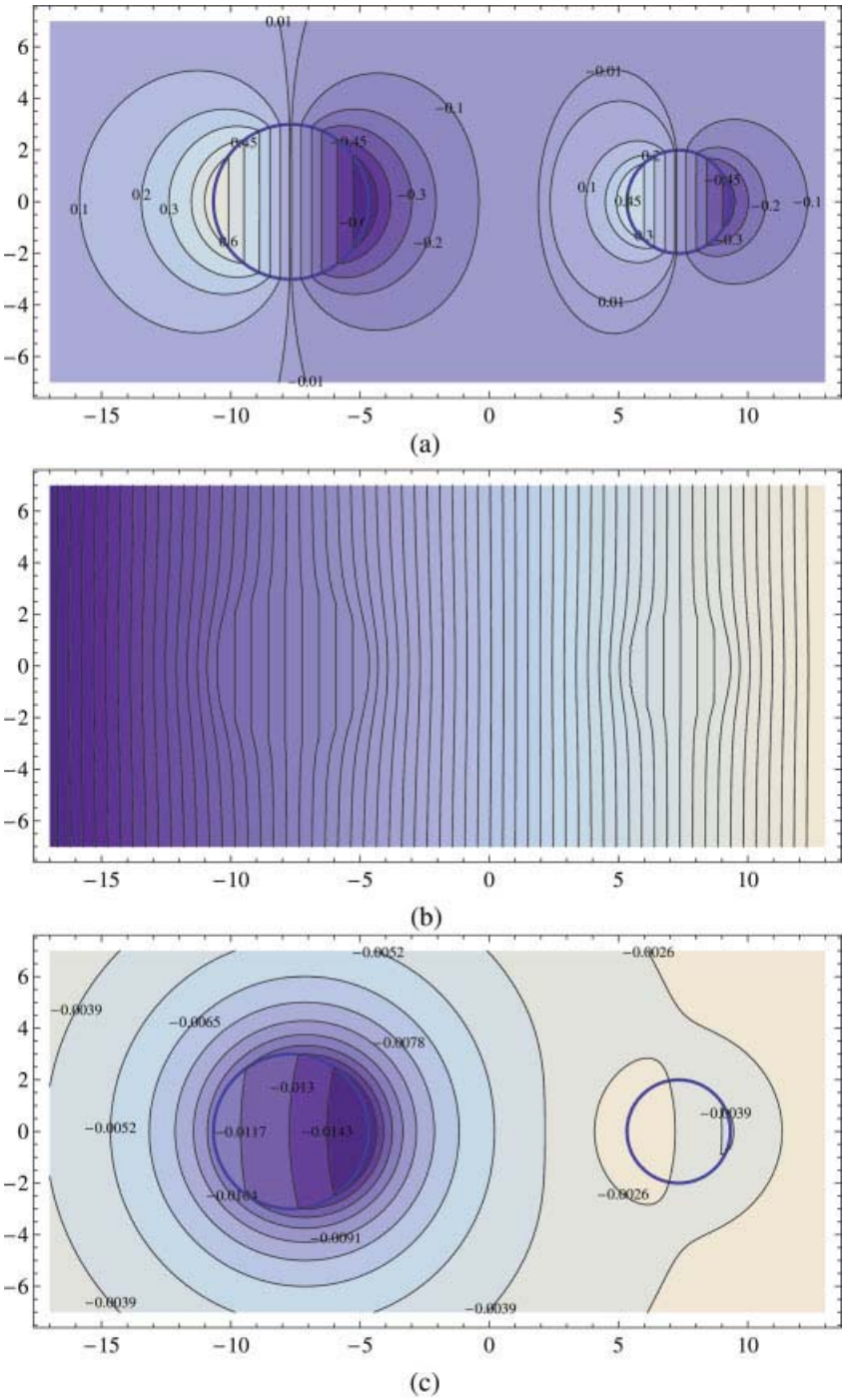

FIG. 4. Contour plots in the plane y_3, y_1 for the case 1 of two well-separated spheres under longitudinal temperature gradient. (a) Perturbation, T_2. (b) Full temperature profile including the main gradient, $\boldsymbol{G} \cdot \boldsymbol{x} + T_2$. (c) 'Pure perturbation', S. [Color figure can be viewed in the online issue, which is available at www.interscience.wiley.com.]

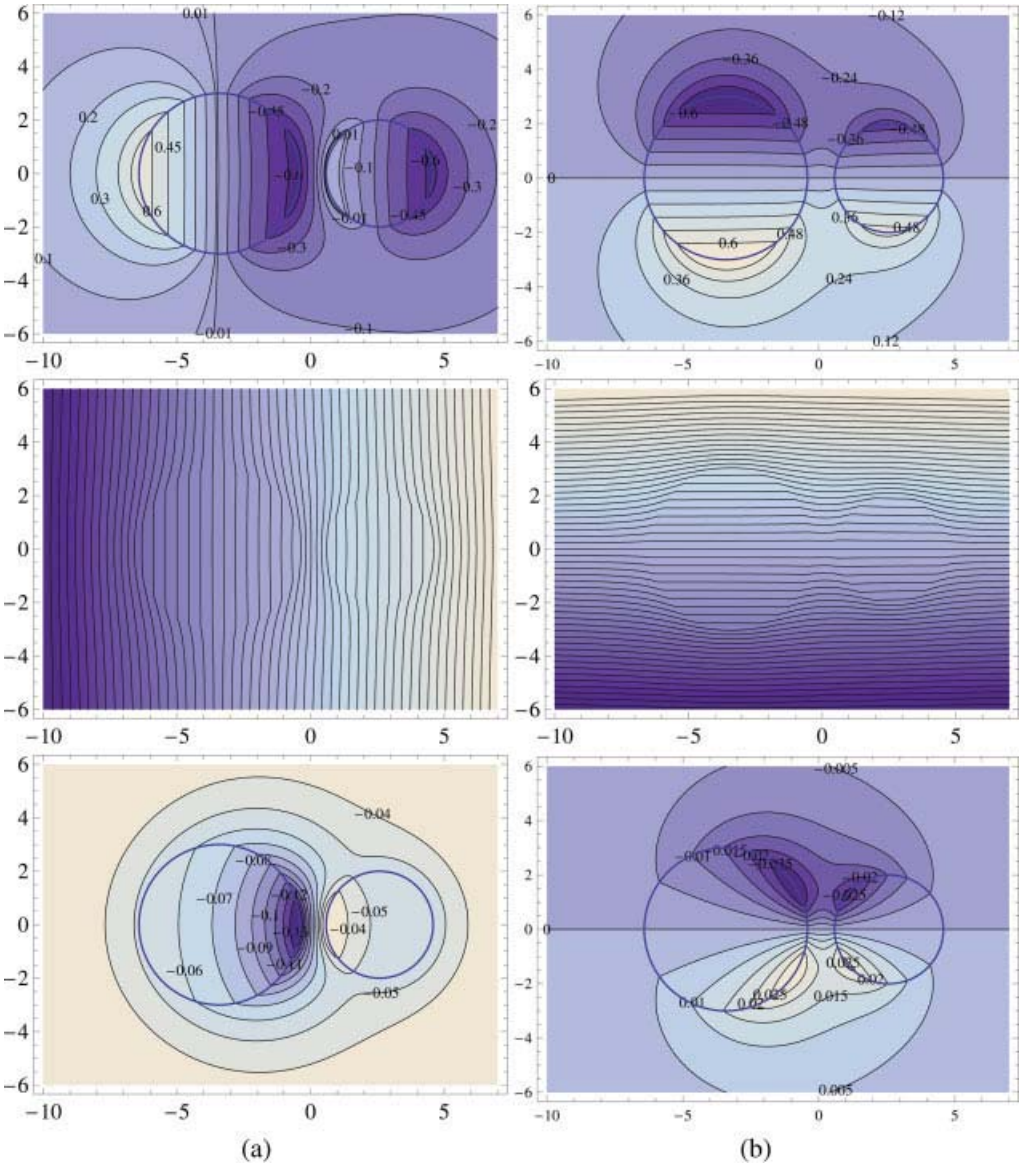

FIG. 5. Contour plots in the plane y_3, y_1 for the case 2 of two closely situated spheres. (a) longitudinal temperature gradient; (b) transverse temperature gradient. [Color figure can be viewed in the online issue, which is available at www.interscience.wiley.com.]

around the axis connecting the centers of spheres. In Fig. 6, we present the results for six different cross-sections of the solution. Now, since the axial symmetry is lost, for different cross sections of $y_2 = \text{const}$, different patterns are observed. It is clear that the disturbance due to the presence of the two spheres must be felt weaker in cross-sections that are far from the line connecting the centers. The first panel in Fig. 6(a) shows the cross-section $y_2 = 0$. The pattern is not symmetric, anymore. In the sequence of plots in the rest of the panels, y_2 gradually increases. When the

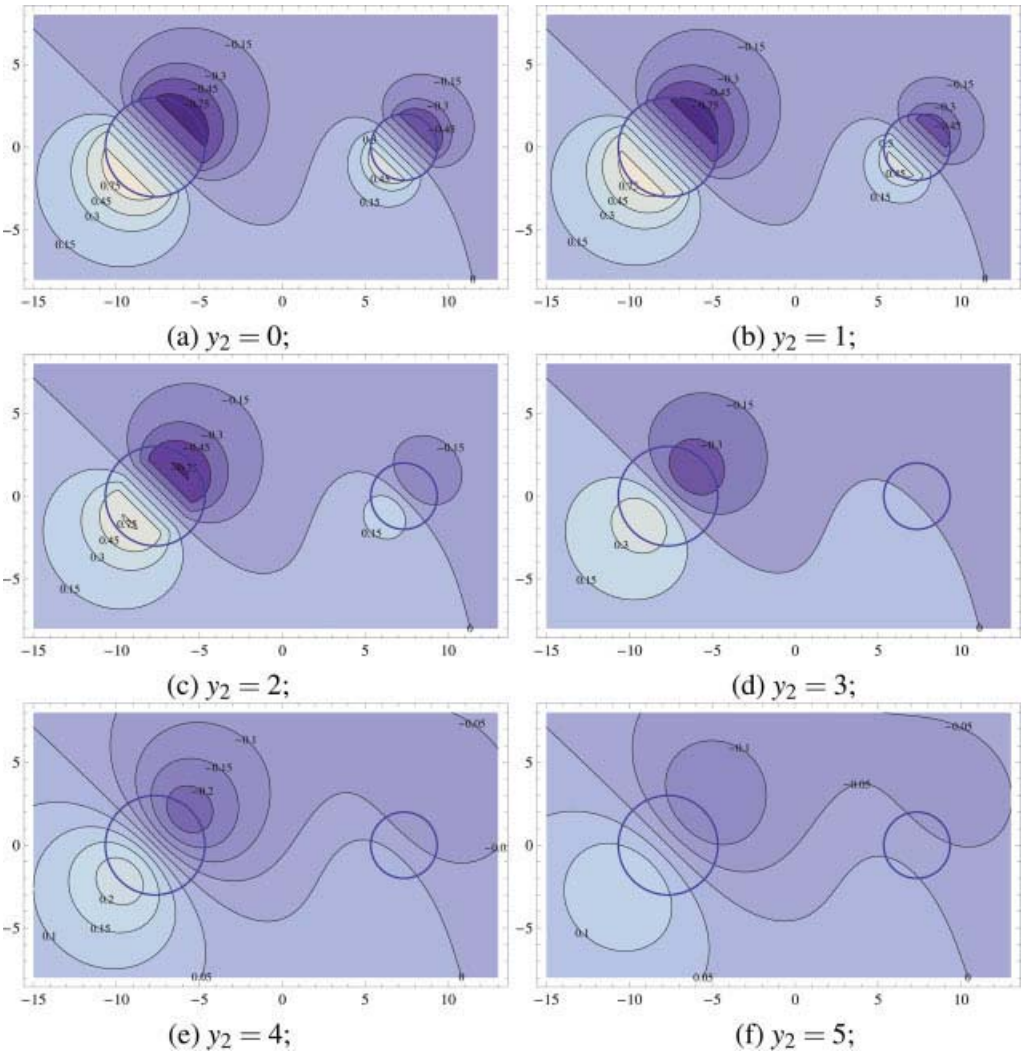

FIG. 6. Case 1. Combined longitudinal $E_3 = 1$ and transverse gradient $E_1 = 1$ at infinity ($E_2 = 0$). Patterns in the plane y_3, y_1 for different planes $y_2 = \text{const}$. [Color figure can be viewed in the online issue, which is available at www.interscience.wiley.com.]

cross-section is at $y_2 = 2$ (equal to the radius of the smaller sphere), the disturbance introduced by the latter is very small. At $y_2 = 3$, the influence of the small sphere is virtually inappreciable and the influence of the larger sphere diminishes in comparison with the cross-sections with smaller y_2. For larger y_2, the plots presented in (e) and (f) show that the disturbance is very small. We choose in (e) and (f) a smaller spacing between the contours, to be able to see the patterns.

In Fig. 7, the same sequence of patterns is presented for the case 2 of the closely situated spheres. Once again, the gradual disappearance of the perturbation with the increase of y_2 is clearly seen.

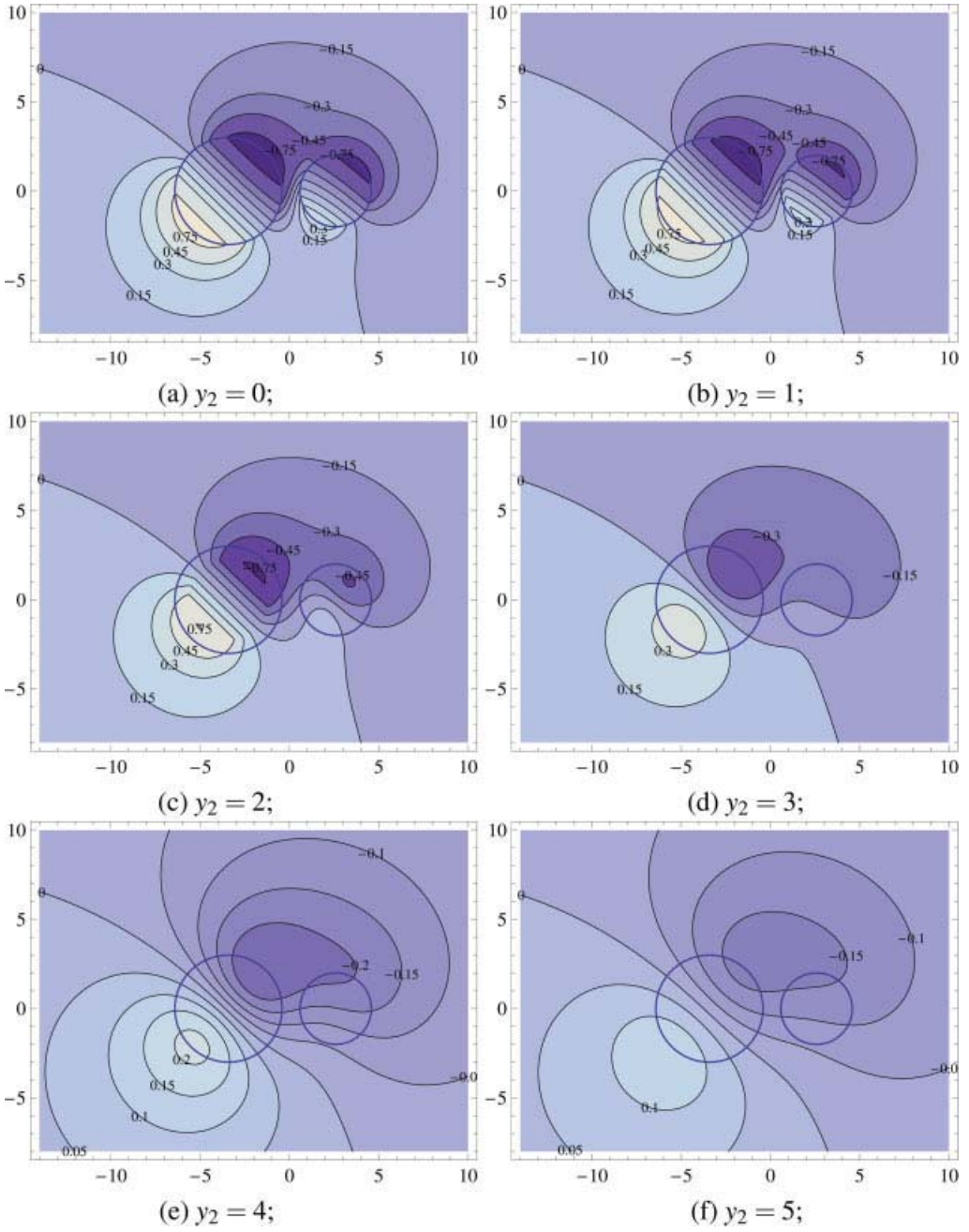

FIG. 7. Case 2. Combined longitudinal $E_3 = 1$ and transverse gradient $E_1 = 1$ at infinity ($E_2 = 0$). Patterns in the plane y_3, y_1 for different planes $y_2 = \text{const}$. [Color figure can be viewed in the online issue, which is available at www.interscience.wiley.com.]

X. CONCLUSIONS

In this article, we solve numerically the problem of temperature distribution around two non-intersecting, unequal spheres, when the temperature field is linear at infinity (constant gradient). Under an arbitrary oriented gradient at infinity, the problem is three-dimensional, and does not allow for analytical solution. We seek the solution in bispherical coordinates for which the spheres are coordinate surfaces. After some substitutions, the problem can be rendered to a problem with separation of the variables. The equation for the coordinate that corresponds to the latitude on a single sphere admits solutions that are Legendre polynomials (e.g., associate Legendre polynomials).

We show that the general solution can be expressed in series in Legendre polynomials. To this end, we use the method of generating functions to expand the boundary conditions into Legendre series and to obtain a closed algebraic system for the coefficients. Thus, a fast spectral method based on expansion in Legendre series of the temperature field is devised, which has exponential convergence. Our numerical results confirm the exponential convergence, and we are able to obtain solutions of accuracy of 10^{-20} with 10–20 terms, which makes the proposed method very efficient.

The solution is thoroughly validated for different distances between the spheres, and shown to be very close to the superposition of two one-sphere solutions when the spheres are separated by a distance twice larger than the sum of their radii.

Various cases are treated and shown graphically for the first time in the literature.

References

1. J. C. Maxwell, A treatise on electricity and magnetism, Clarendon Press, Oxford, 1873.
2. A. Einstein, Eine neue Bestimmung der Moleküldimensionen, Ann Physik 19 (1906), 289–305.
3. L. J. Walpole, The elastic behavior of a suspension of spherical particles, Quart J Mech Appl Math 25 (1972), 153–160.
4. D. J. Jeffrey, Conduction through a random suspension of spheres, Proc Roy Soc A 335 (1973), 355–367.
5. G. K. Batchelor, Sedimentation in a dilute suspension of spheres, J Fluid Mech 52 (1972), 245–268.
6. G. K. Batchelor and J. T. Green, The determination of the bulk stress in a suspension of spherical particles to order c^2, J Fluid Mech 56 (1972), 401–427.
7. R. Herczynski and I. Pienkovska, Toward a statitical theory of suspension, Ann Rev Fluid Mech 12 (1980), 237–269.
8. C. I. Christov, Poisson-wiener expansion in nonlinear stochastic systems, Ann Univ Sof Fac Math Mech, 75 (lb. 2 - Mechanique) (1981), 143–165.
9. C. I. Christov and K. Z. Markov, Stochastic functional expansion for random media of perfectly disordered constitution, SIAM J Appl Math 45 (1985), 289–312.
10. C. I. Christov and K. Z. Markov, Stochastic functional expansion in elasticity of heterogeneous solids, Int J Solids Struct 21 (1985), 1197–1211.
11. C. I. Christov, A further development of the concept of random density function with application to Volterra–Wiener expansions, Comp Rend Bulg Acad Sci 38 (1985), 35–38.
12. C. I. Christov and K. Z. Markov, Stochastic functional expansion for heat conductivity of polydisperse perfectly disordered suspensions, Ann Univ Sof Fac Math Mech, 79 (lb.2 - Mechanique) (1985), 191–207.
13. W. M. Hicks, On the motion of two spheres in a fluid, Phil Trans R Soc London 171 (1879), 445–492.

14. J. Happel and H. Brenner, Low Reynolds number hydrodynamics with special applications to particulate media, Springer, Netherlands, 1983.

15. W. B. Zimmerman, On the resistance of a spherical particle settling in a tube of viscous fluid, Int J Engn Sci 42 (2004), 1753–1778.

16. M. Grammatika and W. B. Zimmerman, Microhydrodynamics of flotation processes in the sea surface layer, 34 (2001), 327–348.

17. S. W. Thomson, Reprint of papers on electrostatics and magnetism, 2nd Ed., McMillan, London, 1884.

18. G. B. Jeffery, On a form of the solution of laplace's equation suitable for problem relating to two spheres, Proc R Soc London A 87 (1912), 109–120.

19. C. I. Christov, Perturbation of a linear temperature field in an unbounded matrix due to the presence of two unequal non-overlapping spheres, Ann Univ Sof Fac Math Mech 78 (lb. 2 - Mechanique) (1985), 149–163.

20. H. Bateman and Erdelyi, Higher transcendental functions, McGraw-Hill, New York, 1953.

21. L. C. Andrews, Special functions for engineers and applied mathematicians, MacMillan, London, 1985.

22. P. J. Davies, Interpolation and approximation, Dover, New York, 1963.